



Contents lists available at ScienceDirect

## Bioorganic &amp; Medicinal Chemistry Letters

journal homepage: [www.elsevier.com/locate/bmcl](http://www.elsevier.com/locate/bmcl)

## Inhibition of bromodomain-containing protein 9 for the prevention of epigenetically-defined drug resistance

Terry D. Crawford<sup>a,\*</sup>, Steffan Vartanian<sup>a</sup>, Alexandre Côté<sup>b</sup>, Steve Bellon<sup>b</sup>, Martin Duplessis<sup>b</sup>, E. Megan Flynn<sup>a</sup>, Michael Hewitt<sup>b</sup>, Hon-Ren Huang<sup>b</sup>, James R. Kiefer<sup>a</sup>, Jeremy Murray<sup>a</sup>, Christopher G. Nasveschuk<sup>b</sup>, Eneida Pardo<sup>b</sup>, F. Anthony Romero<sup>a</sup>, Peter Sandy<sup>b</sup>, Yong Tang<sup>b</sup>, Alexander M. Taylor<sup>b</sup>, Vickie Tsui<sup>a</sup>, Jian Wang<sup>c</sup>, Shumei Wang<sup>a</sup>, Laura Zawadzke<sup>b</sup>, Brian K. Albrecht<sup>b</sup>, Steven R. Magnuson<sup>a</sup>, Andrea G. Cochran<sup>a</sup>, David Stokoe<sup>a,\*</sup>

<sup>a</sup> Genentech Inc., 1 DNA Way, South San Francisco, CA 94080, United States

<sup>b</sup> Constellation Pharmaceuticals, 215 First Street, Suite 200, Cambridge, MA 02142, United States

<sup>c</sup> Wuxi Aptec Co., Ltd., 288 Fute Zhong Road, Waigaoqiao Free Trade Zone, Shanghai 200131, PR China

## ARTICLE INFO

## Article history:

Received 18 April 2017

Revised 19 May 2017

Accepted 20 May 2017

Available online xxxxx

## Keywords:

Epigenetics  
Bromodomain  
BRD9  
Inhibitor  
Resistance

## ABSTRACT

Bromodomain-containing protein 9 (BRD9), an epigenetic “reader” of acetylated lysines on post-translationally modified histone proteins, is upregulated in multiple cancer cell lines. To assess the functional role of BRD9 in cancer cell lines, we identified a small-molecule inhibitor of the BRD9 bromodomain. Starting from a pyrrolopyridone lead, we used structure-based drug design to identify a potent and highly selective in vitro tool compound **11**, (**GNE-375**). While this compound showed minimal effects in cell viability or gene expression assays, it showed remarkable potency in preventing the emergence of a drug tolerant population in EGFR mutant PC9 cells treated with EGFR inhibitors. Such tolerance has been linked to an altered epigenetic state, and **11** decreased BRD9 binding to chromatin, and this was associated with decreased expression of ALDH1A1, a gene previously shown to be important in drug tolerance. BRD9 inhibitors may therefore show utility in preventing epigenetically-defined drug resistance.

© 2017 Elsevier Ltd. All rights reserved.

Bromodomains are a series of 61 different ~110 amino-acid protein modules that recognize acetylated lysine residues on histones as well as on other proteins.<sup>1–7</sup> Significant progress has been made in elucidating the biological function of the bromodomain and extra terminal domain (BET) family consisting of dual bromodomains in bromodomain-containing protein 2 (BRD2), bromodomain-containing protein 3 (BRD3), bromodomain-containing protein 4 (BRD4), and bromodomain testis-specific protein (BRDT).<sup>8,9</sup> However, little is known regarding the biological role of the other bromodomain family members. Because of this, it is important to identify potent and selective bromodomain inhibitors for cellular phenotypic screening in order to elucidate the therapeutic significance of targeting bromodomains for oncology, immunology, and inflammatory diseases. Bromodomain-containing protein 9 (BRD9) is one such non-BET bromodomain, and inhi-

bitors of BRD9 have been disclosed recently.<sup>10–13</sup> Herein we report our discovery of novel inhibitors of BRD9.

While the function of BRD9 is unknown, over-expression has been observed for several disease tissues. The gene encoding BRD9 is located on the 5p arm of chromosome 5 and is over-expressed in cervical cancer as well as non-small cell lung cancer.<sup>14,15</sup> Proteomic analysis has also identified BRD9 as a dedicated member of the mammalian SWI/SNF complex, which has been postulated as being involved in tumor suppression.<sup>16</sup> Finally, Hohmann, et al. have disclosed that BRD9 may play a role in hematopoietic cancers and have used a combination of protein engineering and inhibitor studies to validate the bromodomain as a target.<sup>17</sup>

To further understand the functional role of BRD9, we sought an in vitro BRD9 bromodomain inhibitor tool compound. Our goal was to achieve <100 nM cellular potency against BRD9, while maintaining at least 100-fold selectivity over bromodomain family members in our internal panel of fluorescence resonance energy transfer (FRET) assays. We also sought BRD4 FRET activity > 10 μM to ensure that any phenotypic readout at full BRD9 target coverage would not be obscured by the broad cellular activities observed for

\* Corresponding authors at: Calico Life Sciences, 1170 Veterans Blvd, South San Francisco, CA 94080, United States (D. Stokoe).

E-mail addresses: [terrydc@gene.com](mailto:terrydc@gene.com) (T.D. Crawford), [dhstokoe@calicolabs.com](mailto:dhstokoe@calicolabs.com) (D. Stokoe).

BET inhibitors. The BRD4 bromodomains served as a surrogate for all BET bromodomains due to the high degree of sequence identity among BET family members.

We recently reported the identification of compound **1**, a fragment-derived BRD9 small-molecule lead (Fig. 1).<sup>18</sup> Importantly, this molecule incorporates a highly ligand-efficient pyrrolopyridone core that forms a two-point hydrogen bonding interaction with the conserved asparagine N100 (PDB Code: 5I7Y, 1.45 Å).<sup>18</sup> The *N*-crotyl substituent extending from the pyridone induces a hydrophobic channel adjacent to the conserved binding-pocket water network and conveys significant selectivity for BRD9 over the majority of the bromodomain family.

Lead-optimization efforts targeted substitution along multiple vectors from compound **1**. Structural analysis of **1** bound to BRD9 indicated significant accessible volume extending from the para position of the benzamide deeper into the ZA channel. Also, we believed there was an opportunity to occupy a small pocket formed by the Gly43–Phe44–Phe45 lipophilic shelf in BRD9 by introduction of small substituents at either the meta or ortho position of the benzamide. While potentially beneficial to BRD9 potency, we believed substitution would also result in an unfavorable interaction with the corresponding WPF shelves found in CECR2, TAF1(2), and BET bromodomains, and thereby improve the selectivity profile. It also appeared possible to introduce functionality at the pyrrolopyridone 2-position, extending toward the BC loop region with a small aliphatic substituent.

As we probed SAR on the 4-phenyl ring, we found that polar substituents at the para position such as 2-propanol **2** or morpholine amide **5** both improved BRD9 potency, while also providing increased selectivity over all bromodomains screened (Table 1). We believe that this may be the result of the ability of the polar functional groups to interact with solvent in the relatively large binding pocket found in BRD9.

We next incorporated a methoxy group at the ortho position of compound **2**, as this would rest in a low energy conformation planar to the phenyl ring and effectively fill the available volume adjacent to the BRD9 lipophilic shelf region. While the terminal methyl may be beneficial for potency, desolvation of the ether oxygen in this lipophilic region may account for the overall BRD9 potency

remaining unchanged. We also hypothesized that the methoxy group would create a steric clash with bromodomains containing the more rigid WPF shelf (TAF1, BRD4, CECR2) and therefore increase the selectivity for BRD9. Indeed, we found the selectivity window for **3** increased at least 5 to 7-fold over most of our internal bromodomain panel. BRD4(1) was an exception, showing only a modest selectivity gain. We believe the retained potency for BRD4(1) may be due to the methoxy group being directed away from the BRD4(1) WPF shelf and into the ZA channel, therefore avoiding the steric clash and subsequent potency loss.

The level of cellular engagement by these early lead compounds was assessed by visualization of the displacement of an inducible ZsGreen fusion protein localized to chromatin that forms aggregation “dots” when displaced.<sup>19</sup> These dots can be quantified in a dose-dependent manner to enable EC<sub>50</sub> determination (Table 1). We found that both the 2-propanol (**3**) and morpholine amide (**5**) substituents have sub-micromolar cellular affinity, making them attractive candidates for initial phenotypic screening.

We profiled **3** and **5** in a 3-day viability assay across a panel of 652 cancer cell lines representing 32 distinct indications. Activity was largely restricted to a subset of lines derived from blood and lymph node (Fig. 2A,B, Supporting Information Tables S1 and S2). Analysis of **3** in a subset of the full panel (125 lines) in a longer 8-day assay did not reveal any additional sensitivities (Fig. 2C, Supporting information Table S3).

To extend assay conditions beyond conventional 2-dimensional growth, we applied **3** to cells plated at low density and allowed to grow for 9 days into single colonies (clonogenic assays). We analyzed 18 cell lines from skin, lung, breast and pancreatic cancers, and noted that two cell lines (PC9 and HCC1954) showed modest sensitivity to **3**, albeit only at high concentrations (Fig. 3A). This is in contrast to sensitivity to the Brd4 inhibitor JQ1,<sup>20</sup> which is extremely potent in this assay (Fig. 3B).

To further extend phenotypic assays to those with known dependence on epigenetic alterations, we tested the ability of BRD9 inhibitors to affect the drug tolerant state of cells treated with growth inhibitory compounds. This drug tolerant population (DTP) is dynamic, transient, and mediated by differences in chromatin state relative to the untreated parental population.<sup>21</sup>

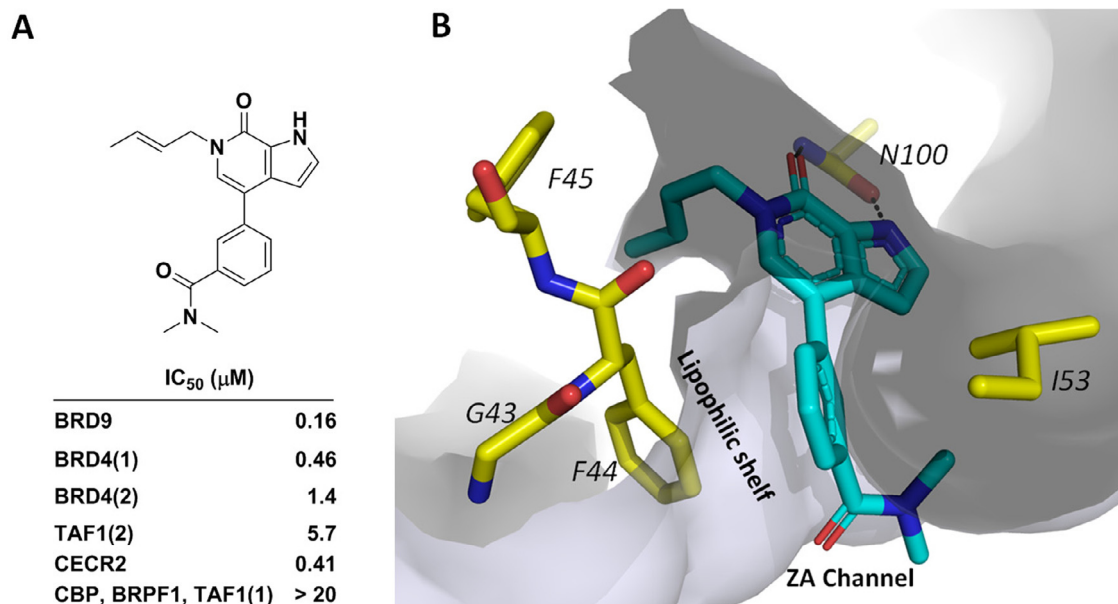


Fig. 1. A) Profile of **1** in biochemical bromodomain binding assays (TR-FRET). IC<sub>50</sub> values are the average from at least 2 independent experiments B) Compound **1** (cyan) bound to BRD9 (residues in yellow). PDB Code: 5I7Y, 1.45 Å.

**Table 1**  
SAR of pyrrolopyridone BRD9 inhibitors.<sup>a</sup>

Compound	R1	R2	Bromodomain TR-FRET (μM)					BRD9 Dot EC50 (μM)
			BRD9	BRD4(1)	BRD4(2)	CECR2	TAF1(2)	
<b>2</b>	H		0.053	3.3 (62x)	6.1 (115x)	4.7 (89x)	5.5 (104x)	0.24
<b>3</b>	H		0.048	5.1	>20	>20	>20	0.19
<b>4</b>	Me		0.008	>20	>20	4.3	>20	0.034
<b>5</b>	H		0.031	3.4	8.3	2.9	1.5	0.38
<b>6</b>	Me		0.012	1.6	6.7	0.81	0.75	0.045
<b>7</b>	Me		0.007	3.5	12.3	0.46	1.4	0.079
<b>8</b>	Me		0.009	6	14.4	1.0	2.8	0.035
<b>9</b>	Me		0.008	4.2	13.5	0.37	0.52	0.031
<b>10</b>	Me		0.006	3.3	17.4	1.0	1.7	0.010
<b>11 (GNE-375)</b>	Me		0.005	>20 (>4000x)	>20 (>4000x)	2.4 (>480x)	>20 (>4000x)	0.013

<sup>a</sup> All bromodomain assays were run in TR-FRET format. IC<sub>50</sub> data are an average of values from at least 2 independent experiments.

Treatment of PC9 cells with 10 μM **3** or **5** alone for eight days had minimal effects on cell viability (Fig. 4A). Erlotinib alone decreased the number of cells by >98%, as expected for PC9 cells (which express the activating EGFR mutant ΔE746-A750 and are dependent upon EGFR activity); the remaining 2% are the DTPs. The histone deacetylase inhibitor Trichostatin A (TSA) does not affect cell growth when used alone; however, in combination with erlotinib, it depletes the drug tolerant persister (DTP) population, leaving no residual surviving cells. When BRD9 inhibitor **3** or **5** was combined with erlotinib, the DTP population was depleted in a dose-dependent manner (Fig. 4B). The BRD4 inhibitor JQ1 was also able to inhibit DTP formation, but, in contrast to BRD9 inhibitors, the high concentration of JQ1 required to deplete the DTPs (Fig. 4B) also decreased viability of PC9 cells in the absence of erlotinib (Fig. 4A).

While the initial biology results were intriguing and suggested a direct role for BRD9 in promoting the appearance of DTP's, we were concerned that these results might not be due to BRD9 inhibition but instead to weak BET family inhibition, as the effects of BRD4 inhibition are highly pleiotropic.<sup>22</sup> While both compounds **3** and **5** were >100-fold selective over BRD4(1), the effects of BET bromodomain inhibition might still be observable at the higher concentrations used in the biological assays (>10 μM). We therefore continued chemistry efforts to limit BRD4 (1 & 2) biochemical potencies to >20 μM while also increasing BRD9 potency. Begin-

ning with the more potent morpholine amide **5**, we focused on substitutions at the 2-position of the pyrrolopyridone, where we predicted that small substituents would be tolerated. Introducing a methyl substituent (**6**) yielded nearly 3-fold biochemical and 8-fold cellular assay potency gains in BRD9; however we also found this potency boost to be a common trend with all bromodomains in our panel (Table 1).

We next explored substitution at the 3-position of the benzamide ring, which we hypothesized would direct away from the lipophilic shelf and further into the ZA channel. Chlorine **7**, methyl **8**, nitrile **9**, and methoxy **10** all provided single-digit nanomolar potencies against BRD9. Methoxy **10** provided the best cellular potency (EC<sub>50</sub> = 10 nM) as well as the best overall selectivity across our bromodomain panel, with the window now 550-fold over BRD4(1), 283-fold over TAF1(2), and 167-fold over CECR2. Finally, we incorporated a 2,5-dimethoxybenzene with both the 2-propanol (**4**) and morpholine amide (**11**) at the 4-position. We hypothesized that this substitution would be well tolerated in BRD9 with the 2-methoxy group occupying the accessible pocket adjacent to the lipophilic shelf, while inducing an unfavorable interaction with BRD4 by forcing one of the two methoxy groups to be directed towards the BRD4 WPF shelf. Gratifyingly, we found that the 2,5-dimethoxy substitution maintained single-digit BRD9 potency for both **4** and **11**, with compound **4** now 540-fold selective over

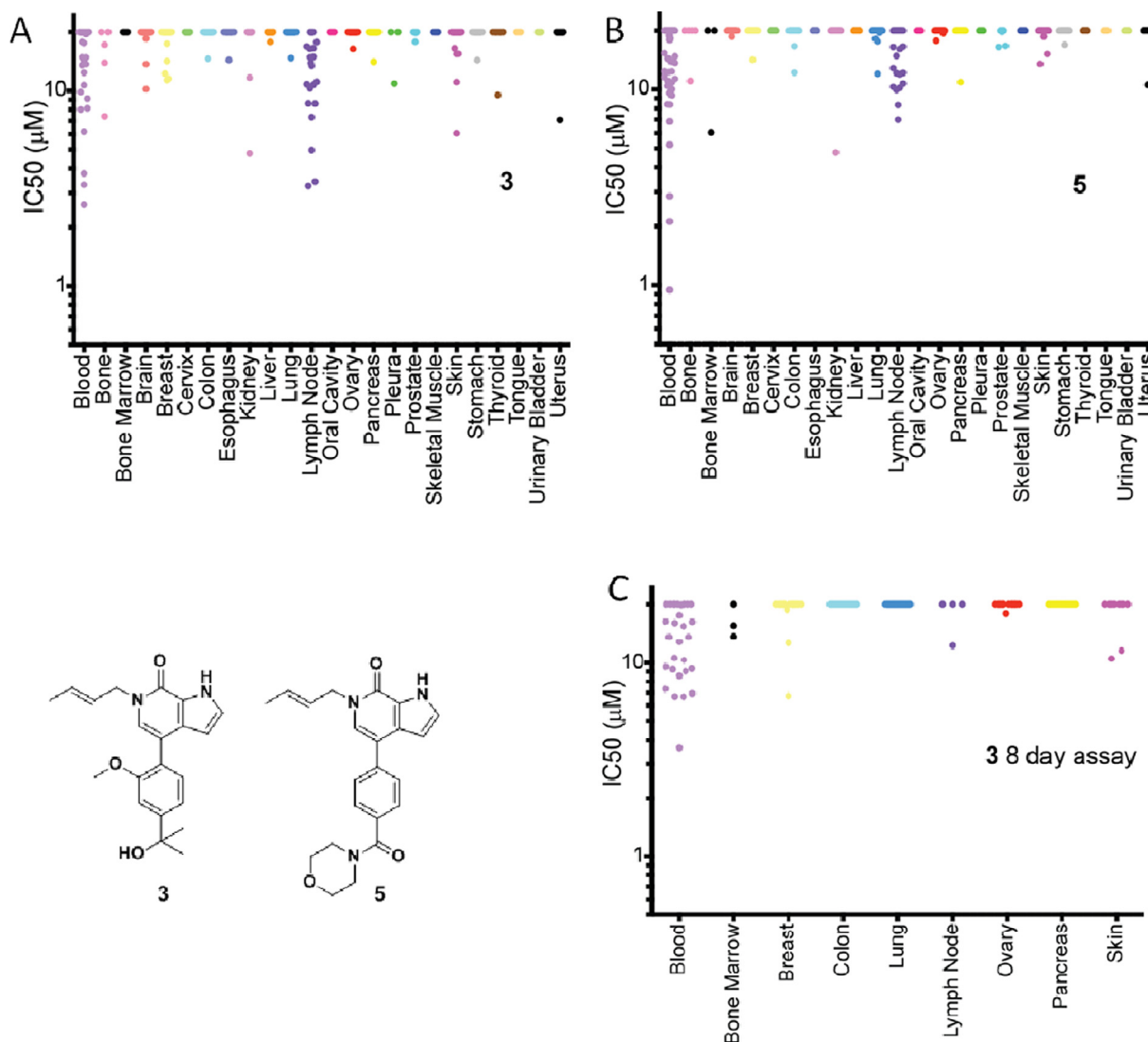


**Fig. 2.** 652 cell lines comprising multiple indications were profiled against **3** (A) and **5** (B) in a 9-point dilution curve using 20 μM as the top concentration. Viability was measured 3 days (A and B) or 8 days (C) following drug treatment using a CellTiter-Glo luminescent assay. IC<sub>50</sub> values on the y-axis are plotted against indication on the x-axis.

CECR2 and >2500-fold selective over the remaining enzymes in the panel, while compound **11** was 480-fold selective over CECR2 and >4000-fold selective against all the other targets we tested. Compounds **4** and **11** also maintained low nanomolar activity in the BRD9 cellular target engagement assay, with EC<sub>50</sub>s of 34 and 13 nM respectively.

To further evaluate the selectivity of this series across bromodomain and non-bromodomain proteins, compounds **3–5** and **11** were profiled in a BROMOscan panel of 40 bromodomains (Supporting Info Fig. S1, Table S4). Surprisingly, we observed nanomolar potency toward GCN5L2 when incorporating the 2-propanol functionality ( $K_D = 410$  nM for **3**, 160 nM for **5**), while no activity was observed with the morpholine amide. Additionally, it is noteworthy that while potent against GCN5L2, compounds **3** and **5** were inactive against homolog PCAF.<sup>23</sup> Compound **4** unexpectedly retained <10 μM binding to several BET family members. Intriguingly, while the mono-methoxy compounds **3** and **5** were a modest 10-fold selective for BRD9 over homolog BRD7, the di-methoxy group yielded additional selectivity over BRD7 with both subseries (104-fold for **4**, 55-fold for **11**). Compound **11** not only had exquisite BRD9 potency in the panel ( $K_D = 2$  nM), but was also found to

be selective against the panel, with only BRD7 and CECR2 ( $K_D = 3600$  nM, 1800-fold selectivity) producing measurable  $K_D$ s under 10 μM, while the selectivity over the remaining bromodomains was at least 5000-fold.

Compounds **3**, **5**, and **11** were screened in an Invitrogen panel of 40 kinases at 1 μM as well as a panel of 37 assays at Cerep (Supporting information Tables S5 and S6). Only **5** was found to show kinase inhibition of >20% at 1 μM (JNK1\_α1 = 25%, TrkA = 21%), while compounds **5** and **11** had >20% inhibition at 10 μM in the Cerep panel (PPARγ agonist = 49%, 5-HT2B agonist = 22% for **5**, benzodiazepine agonist = 86% for **11**). Based on the low nanomolar cellular activity, high degree of selectivity, excellent molecular properties (LogD = 2.4 @ pH 7.4, TPSA = 85, molecular weight = 452) and high kinetic solubility (135 μM), compound **11** was identified as our BRD9 in vitro probe compound, **GNE-375**.

To confirm that **11** binds to endogenous BRD9 in cell lysates we used the cellular thermal shift (CETSA) assay, which measures protein denaturation at increasing temperatures in lysates from compound-treated cells.<sup>24</sup> Compound **11** (2 μM) significantly increased the thermal stability of BRD9 (e.g. at 44–50 °C; Fig. 5), but had no effect on BRD4, consistent with in vitro bromodomain profiling.

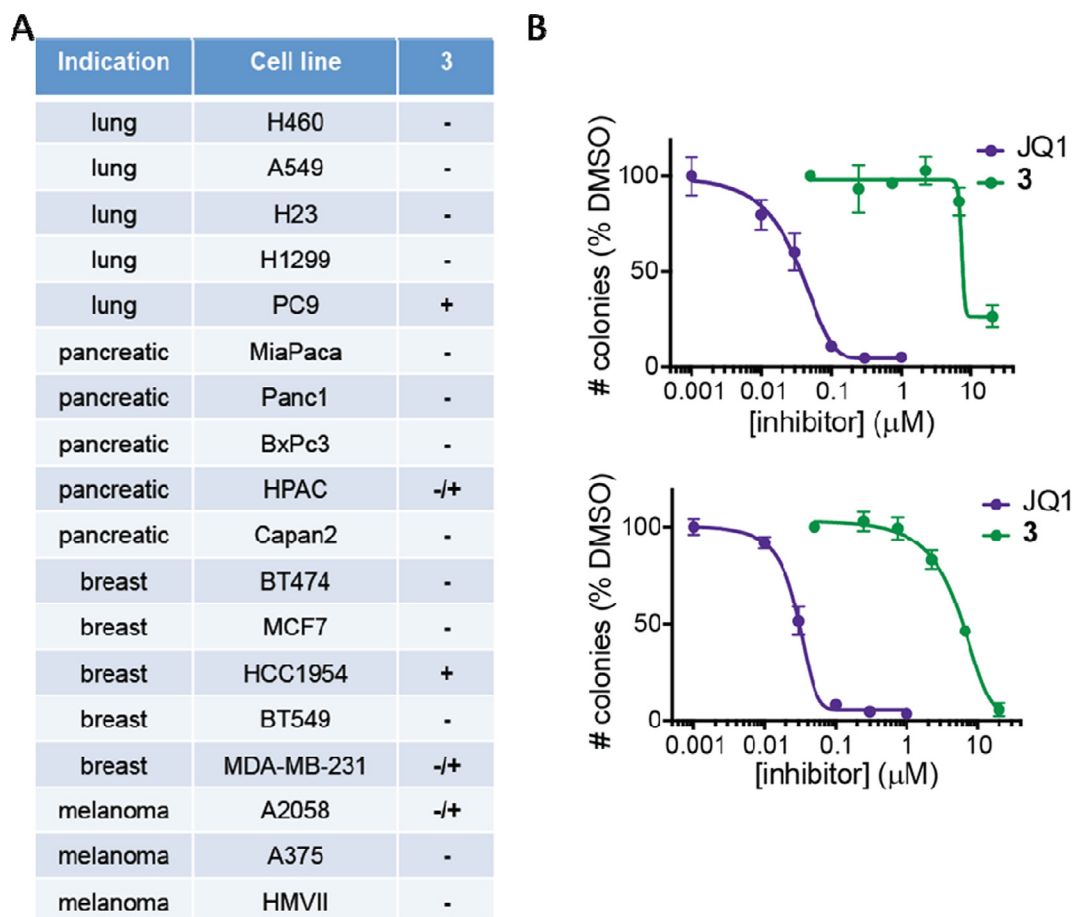


**Fig. 3.** (A) 18 cell lines representing 4 indications were profiled against **3** in a 5-point dilution curve with 20  $\mu\text{M}$  as the top concentration. Cells were stained nine days following drug treatment with MTT and imaged. Activity is indicated qualitatively by + (strong activity at the highest dose), +/- (weak inhibition at the highest doses) and - (no inhibition at any dose). (B) Number of colonies were quantitated and plotted against inhibitor concentrations for PC9 cells (top graph) and HCC1954 cells (bottom graph). The left-most value for each compound is the number of colonies observed in DMSO.

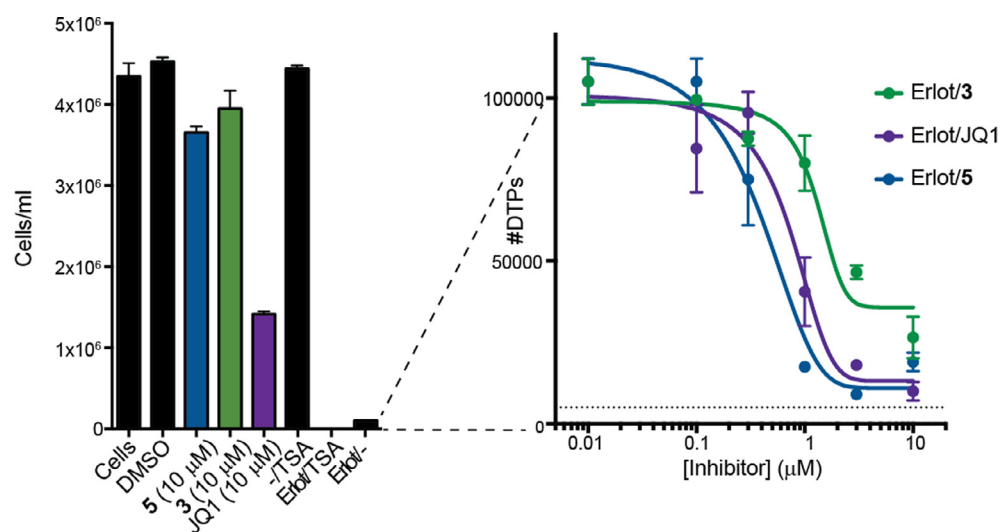


**Fig. 4.** PC9 cells were incubated with the indicated compounds for 3 days, and then cell numbers were counted. Erlotinib was added at 1  $\mu\text{M}$  and TSA was added at 50 nM. The right-hand graph shows a dose response of bromodomain inhibitors added at the same time as 1  $\mu\text{M}$  erlotinib, and cells counted nine days later. The dashed line indicates the expansion of the y axis between the two graphs, and the dotted line represents the number of cells remaining nine days after erlotinib and 50 nM TSA. Error bars represent standard deviations,  $N = 3$ .

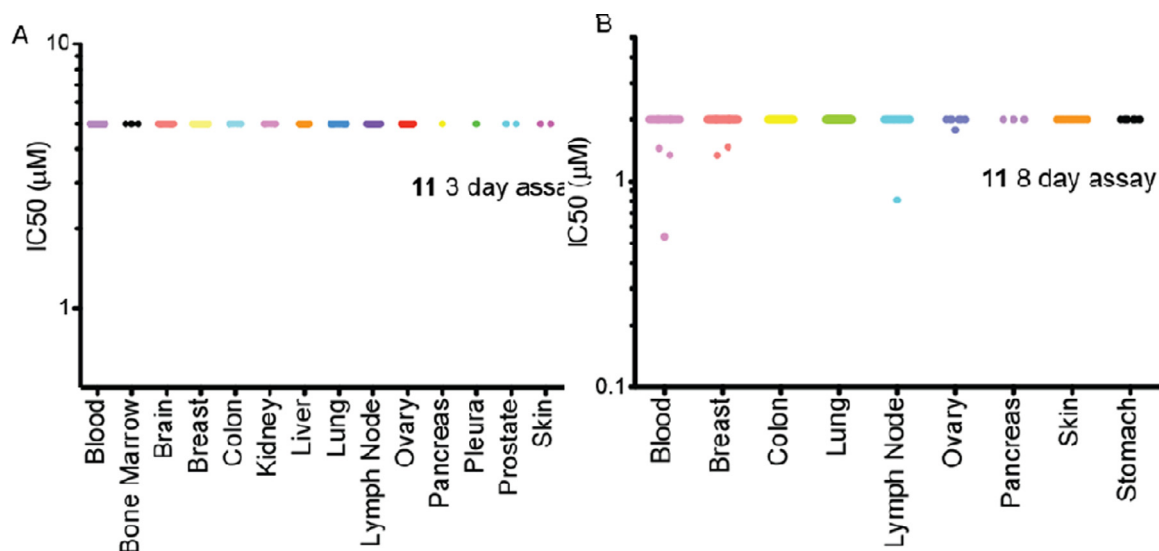


**Fig. 5.** 236 cell lines (A) or 254 cell lines (B) comprising multiple indications were profiled against **11** in a 9-point dilution curve using 5  $\mu\text{M}$  (A) or 2  $\mu\text{M}$  (B) as the top concentration. Viability was measured 3 days (A) or 8 days (B) following drug treatment using a CellTiter-Glo luminescent assay.  $\text{IC}_{50}$  values on the y-axis are plotted against indication on the x-axis.

Conversely, JQ1 (10  $\mu\text{M}$ ) showed strong thermostabilization on BRD4 but had no effect on BRD9 (full temperature range shown in Fig. S2A).

Because of the enhanced selectivity properties of **11**, we revisited the phenotypic effects of BRD9 inhibition in cells. Using a smaller panel of 236 cell lines, **11** showed no activity in any cell line tested, even in the 78 blood and lymph node lines tested in the experiments shown in Fig. 2 (Fig. 5A, Table S7). This suggests that the activities of **3** and **5** in this assay were off-target (likely due to BRD4 inhibition). In an extended 8-day viability assay, activity was restricted to a very small number of cell lines (Fig. 5B, Table S8). Consistent with reduced cellular activity, **11** was also inactive in the clonogenic assay in PC9 and HCC1954 cells (Fig. S3).

Next we tested whether the more selective BRD9 inhibitor retained the ability to suppress DTP numbers following erlotinib treatment in PC9 cells. **11** showed no growth inhibition of the

parental PC9 cells (Fig. 6A), but caused >60% reduction in the number of DTPs when co-dosed with erlotinib, showing increased potency relative to **5**, consistent with its in vitro properties (Fig. 6B). We examined the effects of inhibitor treatment on the expression and localization of BRD9 in parental and drug-tolerant cells. The overall levels of BRD9 do not change in the drug-resistant population. However, BRD9 shows redistribution to the nuclear and chromatin fractions in the DTP population, which is partially prevented if the cells are pre-treated with **11** (Fig. S2B).

Finally, to understand the consequences of BRD9 inhibition that might contribute to its effects on DTP formation, we performed RNAseq analysis of gene expression following 24 h treatment with the BRD9 inhibitors **3**, **4**, **5**, and **11**. Overall the gene expression changes in response to BRD9 inhibitors were modest (Table S9 and Fig. S4). Compounds **3** and **5** inhibited the expression by >2-fold of a relatively small number of genes in the drug-tolerant

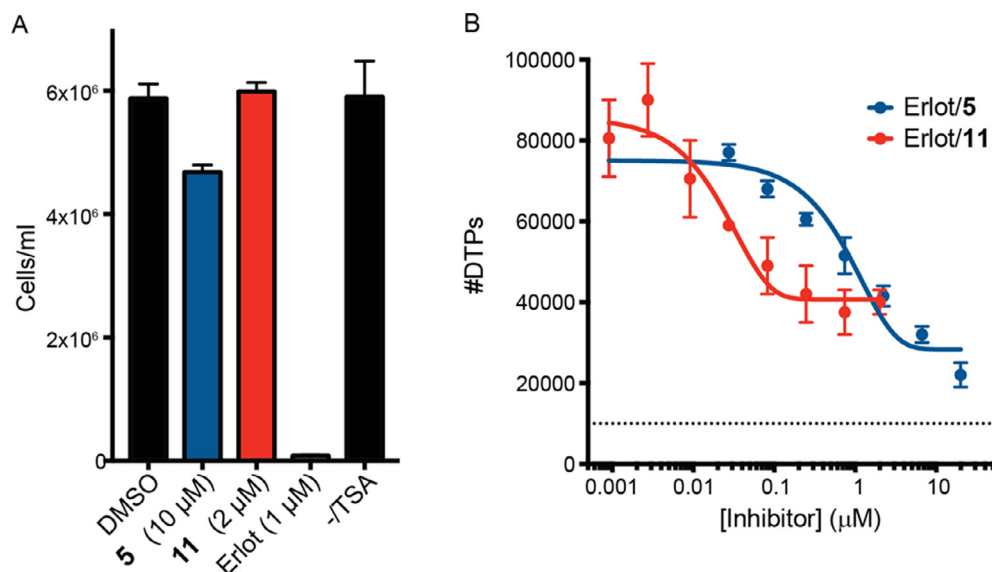


**Fig. 6.** (A) PC9 cells were incubated with the indicated compounds for 3 days, and then cell numbers were counted. (B) Compounds **5** and **11** were added to PC9 cells together with 1  $\mu\text{M}$  erlotinib, and cells counted nine days later. The dotted line represents the number of cells remaining nine days after erlotinib and 50 nM TSA. Error bars represent standard deviations,  $N = 3$ .

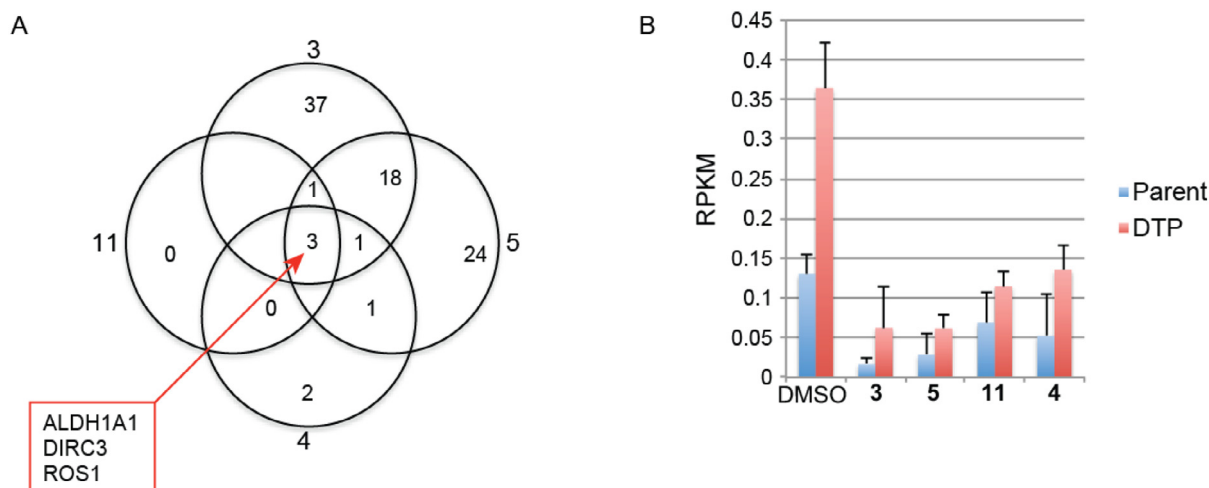


**Fig. 7.** (A) Venn diagram showing the number of genes down-regulated >2-fold in DTPs treated with the indicated compounds. (B) mRNA expression of ALDH1A1 in parental cells and DTPs in untreated (DMSO) and BRD9 inhibitor treated cells. Error bars represent standard deviations, N = 3.

population (59 and 48 respectively), whereas **4** and **11** only inhibited 4 and 7 genes respectively, confirming the increased selectivity of the later compounds. Interestingly, ALDH1A1 was one of only three genes commonly down-regulated by all four BRD9 inhibitors in the drug-tolerant population (Fig. 7A). ALDH genes in general, and ALDH1A1 in particular, have previously been shown to be important for the drug-tolerant phenotype.<sup>25</sup> Fig. 7B shows that this gene is down-regulated by BRD9 inhibitors in both parental and drug-resistant population.

Selective engagement of the BRD9 bromodomain appears to have minimal consequences on gross cell morphology or viability in most cell lines. Only a small subset of leukemia cell lines showed any effect at concentrations <2  $\mu$ M, a concentration >100-fold higher than needed for cellular target engagement. Viability consequences were also only seen in longer-term (8-day) assays, and were not apparent after 3-day treatments, an observation in accord with one made previously.<sup>17</sup> While the effects on cell viability and colony growth using our earlier BRD9 inhibitors were likely due to residual BRD4 inhibition, the effects on drug tolerance remained potent using highly selective BRD9 inhibitors. Therefore, exquisite selectivity over BRD4 is needed to dissect out BRD9-specific functions, as previously suggested.<sup>26</sup>

Genetic alterations such as EGFR T790M are present in a minor fraction (1 in ~50,000 cells) of the parental population of PC9 cells, and underlie a rapid resistance mechanism to 1st generation EGFR inhibitors such as erlotinib. In addition, this mutation in EGFR, as well as mutations in additional genes, can also emerge de novo following drug treatment, which account for a slower resistance to EGFR inhibitors.<sup>27</sup> However, the nine day assay used here captures short-term drug tolerant cells which are independent of these genetic alterations, and instead are predominantly due to epigenetic changes in H3K4, H3K9 and H3K27 methylation.<sup>21</sup> Therefore, it was not unexpected that compounds regulating epigenetic targets might show a response in this model. It will be interesting to see if and how compounds inhibiting epigenetic mechanisms interact with the long term genetic resistance mechanisms such as EGFR mutation, KRas, NRas, BRaf and Ret mutations, as well as met amplification or small cell differentiation.<sup>28</sup>

RNAseq experiments showed only very small changes in gene expression following treatment with these inhibitors. No genes were altered >2-fold in parental PC9 cells, and only 3 genes were commonly down-regulated in the erlotinib-resistant population. Of these, ALDH1A1 is of particular interest, as its levels and activity were previously shown to be increased in crizotinib resistant

gastric cancer cell lines.<sup>25</sup> Moreover, inhibition of total ALDH activity using disulfiram showed no effect on parental cells, but reduced the drug-tolerant population following treatment with crizotinib, similar to the effects seen with BRD9 inhibition. The consequences of disulfiram were also seen using PC9 cells and erlotinib treatment. These observations beg the question: How might BRD9 be regulating ALDH1A1 expression? Both ALDH1A1 itself,<sup>29</sup> as well as its promoter<sup>30</sup> are regulated by acetylation, suggesting that BRD9 could be involved in either or both of these mechanisms.

The other two genes regulated by BRD9 in this system are ROS1 and DIRC3. ROS1 levels have not previously been linked to EGFR inhibitor resistance, but recurrent activating fusions of ROS1 are found in lung cancer, and resistance to ROS1 inhibitors in these settings can occur via a switch to EGFR dependency.<sup>31</sup> Therefore, ROS1 and EGFR show important cross-talk in lung cancer progression and therapy. Much less is known about DIRC3, a lncRNA that was identified as a translocation gene in renal cancer.<sup>32</sup> However, polymorphisms near this gene are associated with breast and thyroid cancer.<sup>33,34</sup>

In conclusion, starting from lead compound **1** we utilized structure-based drug design to target a potent and selective BRD9 inhibitor. Targeted interactions with the lipophilic shelf as well as substitution further into the ZA channel provided optimal potency and greatly enhanced selectivity over the bromodomain family, ultimately resulting in the identification of an in vitro tool compound (Compound **11**, **GNE-375**) suitable for probing the cellular consequences of BRD9 bromodomain engagement. In addition, we have uncovered a previously unknown role of BRD9 in mediating drug tolerance, which could be a useful avenue to pursue for future therapeutic intervention strategies.

## Acknowledgements

We would like to thank the Genentech DNA/RNA sequencing, gCell (cell culture) and gCSI (drug screening) core facilities. Mengling Wong, Michael Hayes, and Amber Guillen are acknowledged for compound purification, and Baiwei Lin, Yanzhou Liu, Deven Wang, and Yutao Jiang for analytical support. Grady Howes, Jan Seerveld, Hao Zheng, Ted Peters, Gigi Yuen, Jeff Blaney, Phil Bergeron, and Thomas Pillow for help with compound management, logistics and technical support are also recognized. We would also like to thank Shiva Malek and Jeff Settleman for helpful advice throughout this study.

## A. Supplementary data

Supplementary data associated with this article can be found, in the online version, at <http://dx.doi.org/10.1016/j.bmcl.2017.05.063>.

## References

- Gershey EL, Vidali G, Allfrey VG. Chemical studies of histone acetylation. The occurrence of epsilon-N-acetyllysine in the f2a1 histone. *J Biol Chem.* 1968;243:5018–5022.
- Haynes SR, Dollard C, Winston F, Beck S, Trowsdale J, Dawid IB. The bromodomain: a conserved sequence found in human, Drosophila and yeast proteins. *Nucleic Acids Res.* 1992;20:2603.
- Winston F, Allis CD. The bromodomain: a chromatin-targeting module? *Nat Struct Biol.* 1999;6:601–604.
- Choudhary C, Kumar C, Gnad F, et al. Lysine acetylation targets protein complexes and co-regulates major cellular functions. *Science.* 2009;325:834–840.
- Sanchez R, Zhou MM. The role of human bromodomains in chromatin biology and gene transcription. *Curr Opin Drug Discov Devel.* 2009;12:659–665.
- Dhalluin C, Carlson JE, Zeng L, He C, Aggarwal AK, Zhou MM. Structure and ligand of a histone acetyltransferase bromodomain. *Nature.* 1999;399:491–496.
- Filippakopoulos P, Picaud S, Mangos M, et al. Histone recognition and large-scale structural analysis of the human bromodomain family. *Cell.* 2012;149:214–231.
- Romero FA, Taylor AM, Crawford TD, Tsui V, Cote A, Magnuson S. Disrupting acetyl-lysine recognition: progress in the development of bromodomain inhibitors. *J Med Chem.* 2016;59:1271–1298.
- Brand M, Measures AR, Wilson BG, et al. Small molecule inhibitors of bromodomain-acetyl-lysine interactions. *ACS Chem Biol.* 2015;10:22–39.
- Theodoulou NH, Bamborough P, Bannister AJ, et al. Discovery of I-BRD9, a selective cell active chemical probe for bromodomain containing protein 9 inhibition. *J Med Chem.* 2016;59:1425–1439.
- Martin LJ, Koegl M, Bader G, et al. Structure-based design of an in vivo active selective BRD9 inhibitor. *J Med Chem.* 2016;59:4462–4475.
- Clark PG, Vieira LC, Tallant C, et al. LP99: discovery and synthesis of the first selective BRD7/9 bromodomain inhibitor. *Angew Chem Int Ed Engl.* 2015;54:6217–6221.
- Hay DA, Rogers CM, Fedorov O, et al. Design and synthesis of potent and selective inhibitors of BRD7 and BRD9 bromodomains. *MedChemComm.* 2015;6:1381–1386.
- Kang JU, Koo SH, Kwon KC, Park JW, Kim JM. Gain at chromosomal region 5p15.33, containing TERT, is the most frequent genetic event in early stages of non-small cell lung cancer. *Cancer Genet Cytogenet.* 2008;182:1–11.
- Scotto L, Narayan G, Nandula SV, et al. Integrative genomics analysis of chromosome 5p gain in cervical cancer reveals target over-expressed genes, including Droscha. *Mol Cancer.* 2008;7:58.
- Kadoch C, Hargreaves DC, Hodges C, et al. Proteomic and bioinformatic analysis of mammalian SWI/SNF complexes identifies extensive roles in human malignancy. *Nat Genet.* 2013;45:592–601.
- Hohmann AF, Martin LJ, Minder JL, et al. Sensitivity and engineered resistance of myeloid leukemia cells to BRD9 inhibition. *Nat Chem Biol.* 2016;12:672–679.
- Crawford TD, Tsui V, Flynn EM, et al. Diving into the water: inducible binding conformations for BRD4, TAF1(2), BRD9, and CECR2 bromodomains. *J Med Chem.* 2016;59:5391–5402.
- Ghosh S, Taylor A, Chin M, et al. Regulatory T cell modulation by CBP/EP300 bromodomain inhibition. *J Biol Chem.* 2016;291:13014–13027.
- Panagis F, Qi J, Picaud S, et al. Selective inhibition of BET bromodomains. *Nature.* 2010;468:1067–1073.
- Sharma SV, Lee DY, Li B, et al. A chromatin-mediated reversible drug-tolerant state in cancer cell subpopulations. *Cell.* 2010;141:69–80.
- Shi J, Vakoc CR. The mechanisms behind the therapeutic activity of BET bromodomain inhibition. *Mol Cell.* 2014;54:728–736.
- Yang X-J, Ogryzko VV, Ji Nishikawa, et al. A p300/CBP-associated factor that competes with the adenoviral oncoprotein E1A. *Nature.* 1996;382:319–322.
- Martinez Molina D, Jafari R, Ignatushchenko M, et al. Monitoring drug target engagement in cells and tissues using the cellular thermal shift assay. *Science.* 2013;341:84–87.
- Raha D, Wilson TR, Peng J, et al. The cancer stem cell marker aldehyde dehydrogenase is required to maintain a drug-tolerant tumor cell subpopulation. *Cancer Res.* 2014.
- Demont EH, Bamborough P, Chung CW, et al. 1,3-Dimethyl benzimidazolones are potent, selective inhibitors of the BRPF1 bromodomain. *ACS Med Chem Lett.* 2014;5:1190–1195.
- Hata AN, Niederst MJ, Archibald HL, et al. Tumor cells can follow distinct evolutionary paths to become resistant to epidermal growth factor receptor inhibition. *Nat Med.* 2016;22:262–269.
- Oser MG, Niederst MJ, Sequist LV, Engelman JA. Transformation from non-small-cell lung cancer to small-cell lung cancer: molecular drivers and cells of origin. *Lancet Oncol.* 2015;16:e165–e172.
- Zhao D, Mo Y, Li MT, et al. NOTCH-induced aldehyde dehydrogenase 1A1 deacetylation promotes breast cancer stem cells. *J Clin Invest.* 2014;124:5453–5465.
- Rice KL, Izon DJ, Ford J, Boodhoo A, Kees UR, Greene WK. Overexpression of stem cell associated ALDH1A1, a target of the leukemogenic transcription factor TLX1/HOX11, inhibits lymphopoiesis and promotes myelopoiesis in murine hematopoietic progenitors. *Leuk Res.* 2008;32:873–883.
- Davies KR, Mahale S, Astling DP, et al. Resistance to ROS1 inhibition mediated by EGFR pathway activation in non-small cell lung cancer. *PLoS ONE.* 2013;8:e82236.
- Bodmer D, Schepens M, Eleveld MJ, Schoenmakers EF, Geurts van Kessel A. Disruption of a novel gene, DIRC3, and expression of DIRC3-HSPBAP1 fusion transcripts in a case of familial renal cell cancer and t(2;3)(q35;q21). *Genes Chromosom Cancer.* 2003;38:107–116.
- Dryden NH, Broome LR, Dudbridge F, et al. Unbiased analysis of potential targets of breast cancer susceptibility loci by Capture Hi-C. *Genome Res.* 2014;24:1854–1868.
- Figlioli G, Kohler A, Chen B, et al. Novel genome-wide association study-based candidate loci for differentiated thyroid cancer risk. *J Clin Endocrinol Metab.* 2014;99:E2084–E2092.